Design and Construction of a Sensorless Drive for BLDC Motor Based on Hysteresis Comparator Estimation Method

Shoorangiz Shams Shamsabad Farahani[1*], Alireza Siadatan[2,3]
1-Department of Electrical Engineering, Young Researchers and Elite Club, Islamshahr branch, Islamic Azad University, Islamshahr, Iran.
Email: shams@iiau.ac.ir (Coresponding Author)
2- Department of Electrical Engineering, College of Technical and Engineering, West Tehran Branch, Islamic Azad University, Tehran, Iran.
Email: siadatan@wtiau.ac.ir
3-Visiting Professor, Energy Systems Group, The Edward S. Rogers Sr. Department of Electrical and Computer Engineering, Faculty of Applied Science and Engineering, University of Toronto, Toronto, ON, Canada.
Email: a.siadatan@utoronto.ca

Received: February 2019 Revised: April 2019 Accepted: July 2019

ABSTRACT:
Brushless DC motors face many challenges and complexities which could be considered as sensor-based or sensorless schemes for detecting the position of the rotor, and end in a variety of results. A brushless DC motor sensorless control system is developed in this paper and a sensorless technique which is based on a hysteresis comparator and a potential start-up method with a high starting torque has been suggested. In addition, the phase delay of the back EMFs, in case of passing low-pass filters, could be compensated by the hysteresis comparator which prevents multiple output transitions from ripple or noise in the terminal voltage. The rotor position is aligned at standstill for maximum starting torque without additional sensors and motor parameter information. Where, by modulating the pulse width of the switching devices during alignment, the stator current could be easily adjusted. In this paper, the simulation and the experimental results has been provided for validating the proposed method.

KEYWORDS: Brushless DC Motor (BLDC), Hysteresis Comparator, Sensorless Control, Start-Up Technique.

1. INTRODUCTION

Nowadays, brushless DC motors are of paramount importance due to their long operating life, high efficiency, removal of copper rotor losses, high dynamic response, low content and weight, heat loss reduction, low noise, easy maintenance, higher speed range, higher torque–weight ratio, better speed vs. torque characteristics, removal of brush sparks, elimination of radio frequency interference and simple control. In return, the problem of operation's drive and their operating method without sensors remains as a main problem [1].

Rotor position determination in BLDC motors is necessary to obtain constant torque, torque producing mechanism, phase exciting and drive control [2]. So, motor staring regardless of rotor position is not practical. Generally, in BLDC motors which are equipped by trapezoidal supply, the Hall- effect sensor is used to determine rotor position. However, cost increase, hardware drive complexity and reliability reduction can be considered as the limitations to utilize mechanical sensors especially in high speed motors which require high precision and light rotors. In addition, the reliability decreases regarding sensitivity of sensor in case either the temperature, or mechanical vibrations or pollution are high. In this regard, sensorless methods overcome these restrictions. The equivalent circuit of a sensorless BLDC motor drive with PWM inverter is shown in Fig. 1.

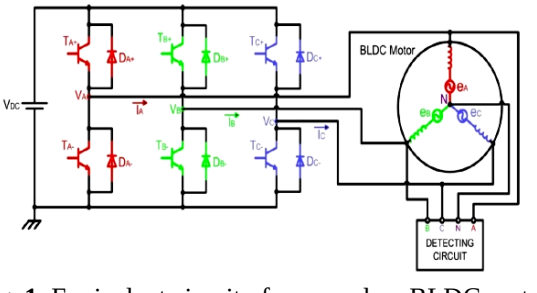

Fig. 1. Equivalent circuit of a sensorless BLDC motor drive with PWM inverter.

Due to the non-sinusoidal back EMF and BLDC motor phase currents, the use of rotary field theory and two-axis conversion are not possible. As a result,

sensorless techniques which are used for motors with sinusoidal supply for BLDC motor are not applicable. Therefore, the BLDC motors are enjoyed techniques to estimate the rotor position and motor speed by measuring voltage or current phase. These methods are categorized into five main groups: methods based on back EMF [3-7], stator flux estimation methods [8], methods with the evaluation and use of stator inductance changes [9], methods with the use of functions in accordance with back EMF [10-12] and methods based on control theories [13-19].

It is necessary to measure the EMF voltage in EMF voltage-based methods. This measurement can be obtained in four ways: EMF voltage or terminal voltage measurement, EMF voltage third harmonic measurement to determine the switching time in sensorless brushless direct current motors, the freewheeling diode current measurement in off-phase and finally, the EMF voltage integration where the commutation time is determined by off-phase voltage integration. This method is based on the integrated EMF voltage over the commutation period which is almost the same for all speed values.

In leakage flux estimation method, flux leakage is achieved based on stator voltage and current, and the rotor position is estimated by curve fitting. However, other methods use the stator inductance changes to estimate the rotor position. There exist some problems in the EMF measurement techniques as voltage and frequency dependence on motor speed, measurement issues and filtering. So, obtaining a proportional function to the EMF voltage which is related to commutation points is of paramount importance. Other methods are observer-based which are suggested in motors with sinusoidal sources. The methods use a mathematical model of brushless direct current motor.

There exist some restrictions in the starting methods of sensorless brushless direct current motor. Specially, EMF voltage and flux leakage estimation have some limitations at low speed area. However, novel digital techniques and measurement methods solve some of the existing problems and render acceptable consequences. Most methods which are based on control theory have low estimation accuracy. Also, the EMF voltage and the stator inductance change approaches have average estimation accuracy and average software and hardware implementation. Table 1 shows the comparison of sensorless methods in BLDC motor drives [20].

Table 1. Comparison of sensorless methods in BLDC motor drives [20].

Comparison							Rotor estimation method	
Estimation accuracy		Possibility of Implementation		Performance				
Transient State	Steady State	Hardware Devices	Software Devices	Rotor Velocity Range (RPM)	High Speed	Low Speed		
Low	Medium	Low	Low	5% ωb-6000	High	Low	**Back EMF Measurement**	**Methods based on Back EMF**
Low	High	Medium	Medium	100-6000	Low	Low	**Third Harmonic Back EMF Measurement**	
Low	High	Very high	Medium	45-10000	High	High	**Freewheeling Diode Flow Measurement**	
Medium	Medium	Medium	Medium	<3600	Medium	Low	**Integrating Back EMF**	
Medium	High	Medium	High	N/A	Medium	Low	**Stator Flux Estimation Methods**	
Medium	Medium	Medium	Medium	>50	Medium	High	**Methods with the Evaluation and use of Stator Inductance Changes**	
Medium	High	Low	Medium	N/A	High	Medium	**Gradient of DC Link Flow Variation**	**Methods using Functions in Accordance to Back EMF**
High	High	Very low	Medium	>1.5% ωb	High	High	**Using Line- Line Flux Function Ratio**	
Low	Medium	High	High	N/A	Medium	Low	**Luenberger Observer**	**Control-Based Methods**
Medium	High	High	Medium	20-150%ωb	High	Medium	**Sliding Mode Observer**	
High	High	High	Very high	1%ωb-105%ωb	Medium	High	**Extended Kalman Filter**	
Low	Medium	High	Very high	100-1200	Medium	Low	**Model Reference Adaptive Systems**	
Low	Medium	High	Very high	N/A	Medium	Low	**Smart Methods**	

This paper develops a sensorless control system for BLDC motor based on a hysteresis comparator with desirable features and performance. The motor prepared for the current study is a BLDC motor built by

Munoz Company with 57BL120L2 model**.** Also, Hall-effect sensor is used to determine rotor position in manufacturing the aforementioned motor. In this method, a sensorless drive is proposed based on hysteresis comparator estimation method to determine the rotor position. In the proposed method, a sensorless drive is considered where the hardware complexity and the motor size are reduced and high reliability is gained. Since the number of transistors is reduced, cost reduction is gained in the proposed method comparing with sensored/sensorless BLDC conventional drives. Also, in this new method, the torque per volume is improved comparing with sensored/ sensorless BLDC conventional drives, so efficiency is improved in the same torque per volume. Also, the motor is able to work in environments with high temperature, humidity and high pollution since it is sensorless.

In this paper, the following items are addressed:

- Design and construction of a brushless dc motor sensorless control system and a sensorless technique based on a hysteresis comparator and a potential start-up method with a high starting torque.
- Compensation of phase delay of the back EMFs in case of passing low-pass filters by the hysteresis comparator to prevent multiple output transitions from ripple or noise in the terminal voltage.
- The rotor position alignment at standstill for maximum starting torque without additional sensors and motor parameter information.
- The stator current adjustment by modulating the pulse width of the switching devices during alignment.
- Providing the simulation and experimental results to verify the validation of the proposed method.

The reminder of this article is as follows: First, sensorless BLDC motor control using the hysteresis comparator is stated. Next, the simulation results and the experimental results are presented, and finally we conclude our study.

2. SENSORLESS BLDC MOTOR CONTROL USING THE HYSTERESIS COMPARATOR

In this section, a novel sensorless BLDC motor control is presented using hysteresis comparator. Fig. 2. illustrates a block diagram of a sensorless controller using the hysteresis comparator which is consisted of low pass filters, the hysteresis comparator and a signal manufacturer. Low pass filters and the hysteresis comparator are used to eliminate high switching frequency ripple and create phase commutation signals, respectively, and the signal manufacturer is utilized to produce six PWM signals [12]. After applying voltage to phases, the high switching frequency ripple and noise are eliminated by input passing through low pass filters. Since only two of three phases in BLDC motors have energy at any time, back EMF can be calculated in off period of 60 degrees. During the transition period of the two phases (120 degrees), the only difference between back EMF and the terminal voltage is stator impedance which does not make much difference with the dc voltage source. Therefore, the terminal voltage waveform is almost the same as the back-EMF voltage waveform. The terminal voltage can be used to find the commutation points in BLDC motors.

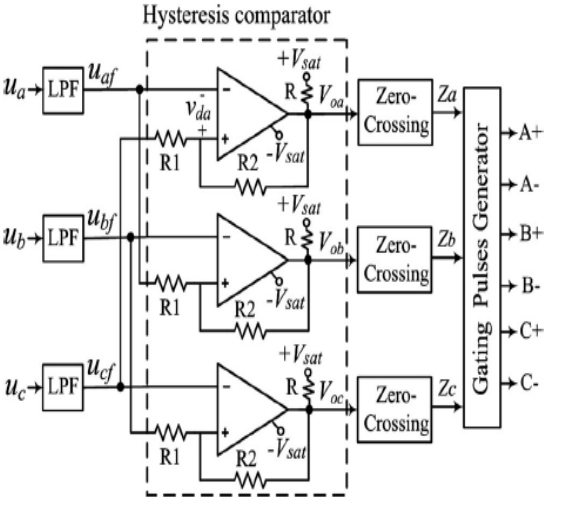

Fig. 2. Block diagram of a sensorless controller using the hysteresis comparator.

The hysteresis comparator is used to compensate the phase delay of the back EMF in case of passing through low-pass filters and chooses the correct commutation area for inverter according to the rotor location. It can prevent multiple output transfer by high frequency ripple in terminal voltage. Three-phase hysteresis comparator output are three commutation signals (Z_a، Z_b، Z_c) which can produce six cut signals by logic calculations. V_{da} as the phase A differential voltage of hysteresis comparator is as follows:

$$V_{da} = -u_{af} + \frac{1}{n+1} V_{oa} + \frac{n}{n+1} u_{cf} \quad (1)$$

Where V_{oa} is the phase A differential voltage of the hysteresis comparator output, n is the resistance ratio $\frac{R_1}{R_2}$, u_{cf} and u_{af} are the phase C and A filtered terminal voltages, respectively.

In case where $V_{oa} = +V_{sat}$,when the differential voltage V_{da} in equation (1) is negative, V_{oa} becomes $-V_{sat}$ and V_{sat} is the output voltage level. For phase C filtered terminal voltage u_{cf} ,we have:

$$u_{cf} \leq \left(\left(1+\frac{1}{n} \right) u_{af} - \left(\frac{1}{n} \right) V_{sat} \right) \quad (2)$$

Also, in $V_{oa} = -V_{sat}$, when the differential voltage V_{da} in equation (1) is positive, V_{oa} becomes $+V_{sat}$. For phase C filtered terminal voltage u_{cf} ,we have:

$$u_{cf} > \left(\left(1+\frac{1}{n} \right) u_{af} + \left(\frac{1}{n} \right) V_{sat} \right) \quad (3)$$

$\left(\frac{1}{n}\right) V_{sat}$ in equations (2) and (3) represents the hysteresis band which is defined by the resistance ratio and the output voltage level V_{sat}. The right side of equations (2) and (3) represent the minimum (V_{LT}) and maximum (V_{UT}) of the phase C terminal voltage respectively, and we have:

$$V_{UT} = \left(1+\frac{1}{n} \right) u_{af} + \left(\frac{1}{n} \right) \quad (4)$$

$$V_{LT} = \left(1+\frac{1}{n} \right) u_{af} - \left(\frac{1}{n} \right) V_{sat} \quad (5)$$

When the output voltage is $+V_{sat}$ and u_{cf} is less than V_{LT}, the output voltage becomes $-V_{sat}$ .Then , as long as u_{cf} is less than V_{LT}, the output voltage remains $-V_{sat}$. Since the main commutation signal Z_a is achieved by the filtered terminal voltage, there exists a difference between Z_a and the correct commutation point. V_{LT} can be represented as follows:

$$V_{LT}(t) = \frac{12V_p}{T_s} \left(1+\frac{1}{n} \right) t - \left(\frac{1}{n} \right) V_{sat} \quad (6)$$

Where T_s and V_p are the terminal voltage period and peak, respectively. Based on (2), t_c as the time between V_p and u_{cf} is obtained as follows:

$$t_c = \frac{T_s}{12} \left(\frac{n}{n+1} + \frac{1}{n+1} \times \frac{V_{sat}}{V_p} \right) \quad (7)$$

t_a as the time delay between $\frac{T_s}{12}$ and t_c is achieved as follows:

$$t_a = \frac{T_s}{12} - t_c \quad (8)$$

Based on equations (7) and (8), the angle θ_a as the phase difference of the three commutation signals from the commutation points estimated by three-phase terminal voltages is derived as follows:

$$\theta_a = \omega t_a = \frac{T_s}{12} \times \frac{1}{n+1} \times \left(1 - \frac{V_{sat}}{V_p} \right) \quad (9)$$

The logic equations to make six cut-off signals from three PWM inverter commutation signals is as follows:

$$\begin{aligned} &A+=(Z_a+Z_b).\overline{Z_a}, \quad A-=(Z_a+Z_b).Z_a \\ &B+=(Z_b+Z_c).\overline{Z_b}, \quad B-=(Z_b+Z_c).Z_b \\ &C+=(Z_c+Z_a).\overline{Z_c}, \quad C-=(Z_c+Z_a).Z_c \end{aligned} \quad (10)$$

According to Equation (10), timing diagram for phase A unfiltered terminal voltage, three-phase commutation signals and cut-off signals proportional to three-phase filtered terminal voltage, is shown in Fig. 3.

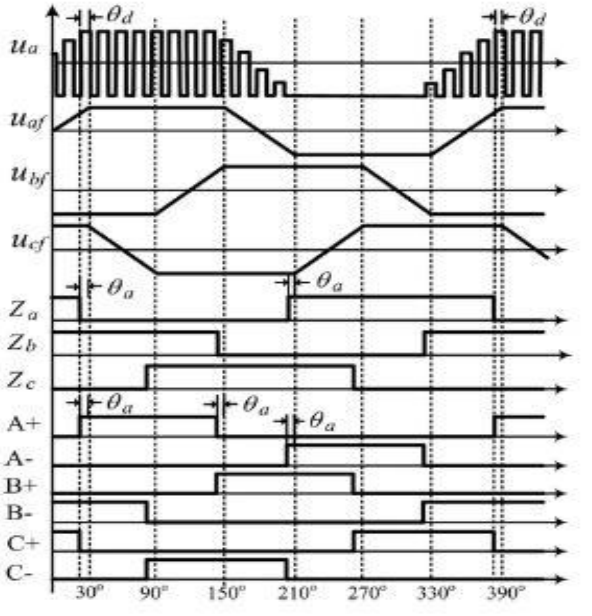

Fig. 3. Timing diagram for phase commutation signals and three phase cut-off signals proportional to terminal voltage.

The filtered terminal voltage of phase A is used to reserve input, and the filtered terminal voltage of phase C with R1 are used to return to the first mode. There exists a difference of θ_d between the filtered terminal voltage of phase A and the unfiltered terminal voltage gain phase. The three commutation signals are θ_a lead from the commutation points estimated by three-phase terminal voltages which can be compensated by low-pass filters. Since the filtered terminal voltage waveform is almost the same as the EMF voltage, the alternative cut-off signal in each inverter bridge phase is in-phase with each EMF voltage phase.

3. THE SIMULATION RESULTS

In this section, BLDC motor is simulated using MATLAB simulator. The parameters considered are as follows:

Table 2. BLDC parameters used in simulation.

Value	Parameter	Value	Parameter
$P_n = 180\ w$	Nominal power	$\omega_n = 300rpm$	Nominal speed
$T_n = 5.7\ N.m$	Nominal torque	$I_n = 4.5\ A$	Nominal current
$K_t = 1.25\ N.m/$	Torque constant	$K_e = 0.0667\ V/rp$	Back EMF constant
$Z = 16$	Number of poles	$R = 0.64$ ohm	Phase resistor
$L_s = 0.1\ mH$	Self-Inductance	$M = 0.25\ mH$	Mutual Inductance

The following results are obtained:

Figs. 4 and 5 show the phase currents and the phase commutation (Phases A, B and C), respectively.

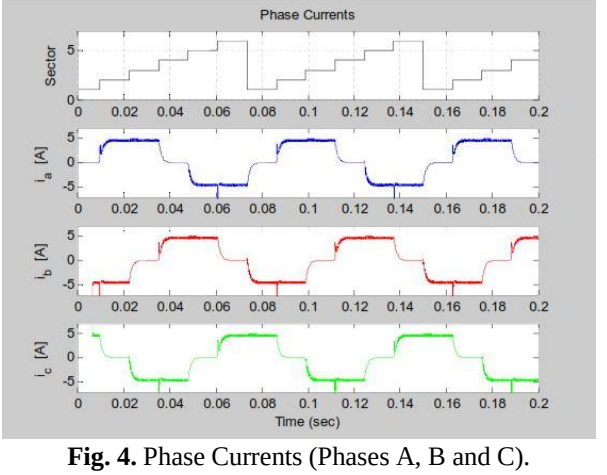

Fig. 4. Phase Currents (Phases A, B and C).

It is clear that the phase currents are changing between -5 to +5 A.

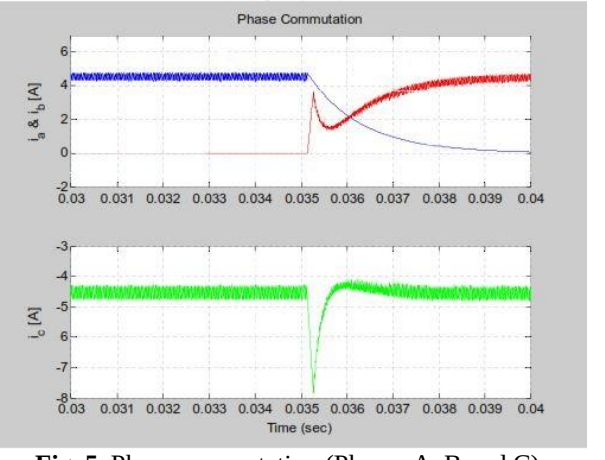

Fig. 5. Phase commutation (Phases A, B and C).

The current and the nominal speed for one phase is shown in Fig. 6.

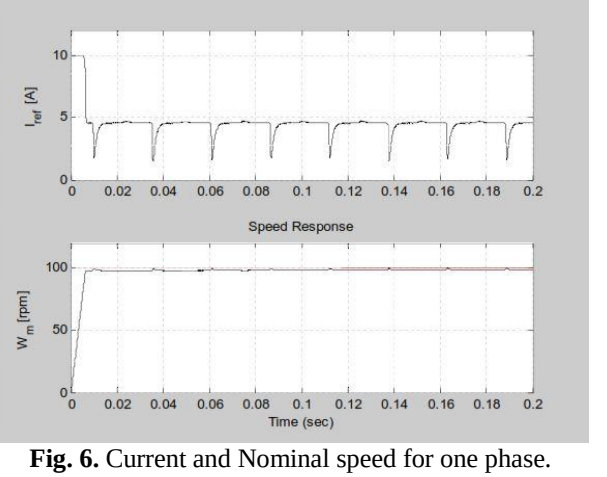

Fig. 6. Current and Nominal speed for one phase.

The phase torque is shown in Fig. 7.

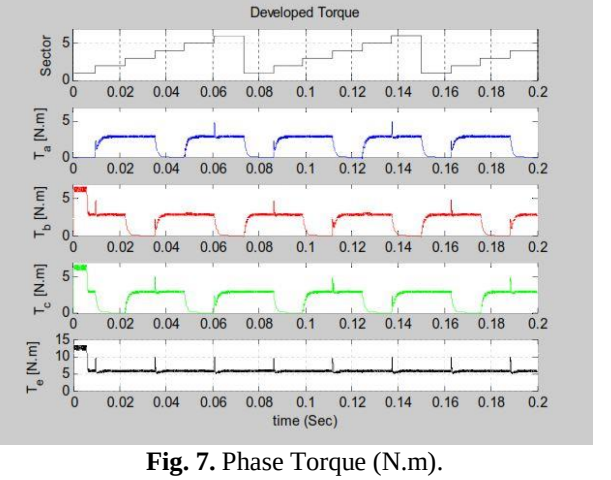

Fig. 7. Phase Torque (N.m).

The phase voltage (Phases A, B and C) is shown in Fig. 8.

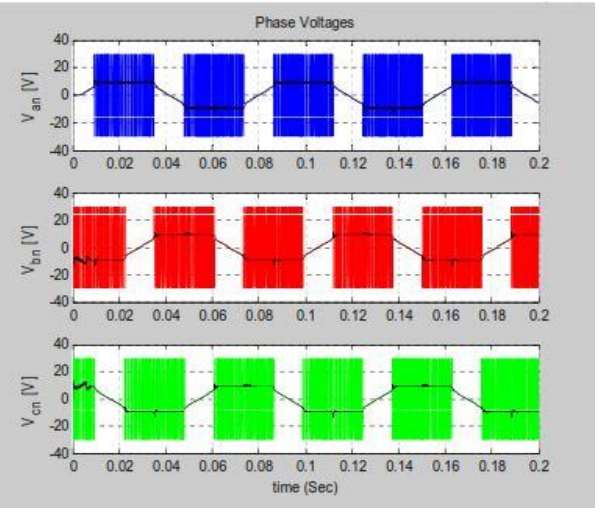

Fig 8. Phase Voltage (Phases A, B and C).

4. THE EXPERIMENTAL RESULTS

After completion of starting-up circuit design and construction, the circuit is set up and tested in the laboratory. By providing a power supply of 24 V, 10 mA and 50 Hz, motor starting-up hardware is completed. Figs. 9 and 10 show the top view of the printed circuit for motor start-up and the starting-up circuit, respectively.

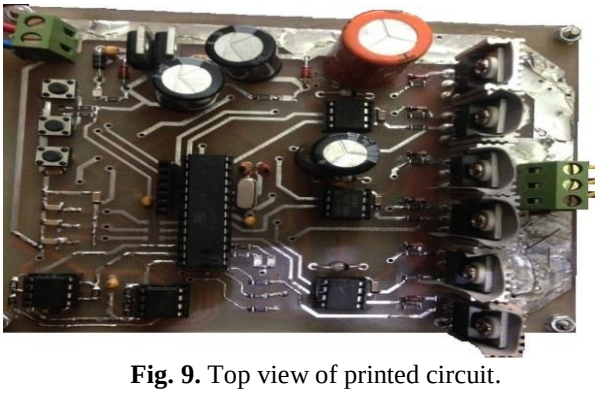

Fig. 9. Top view of printed circuit.

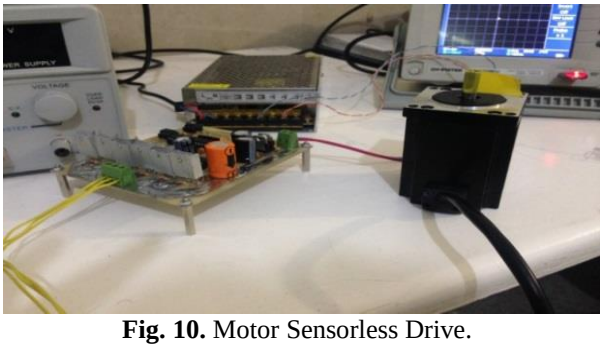

Fig. 10. Motor Sensorless Drive.

Figs. 11-13 show the hysteresis circuit output, voltage of the motor phase and the stator current changes, respectively. It is clear that the Hysteresis circuit output is changing between -5 to +5 and the stator current becomes intermittently positive, negative and zero which is the phase moment charge.

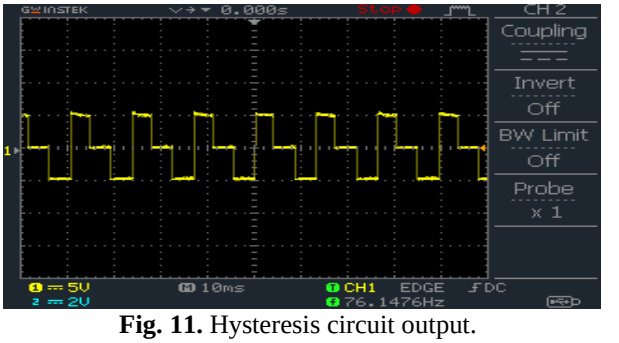

Fig. 11. Hysteresis circuit output.

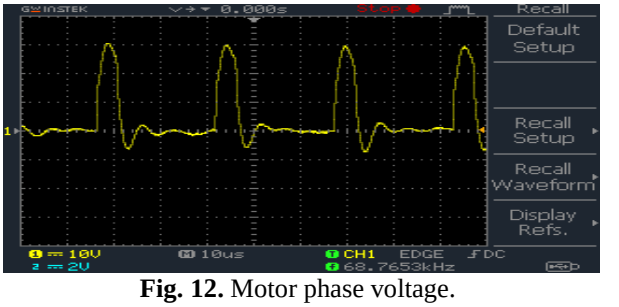

Fig. 12. Motor phase voltage.

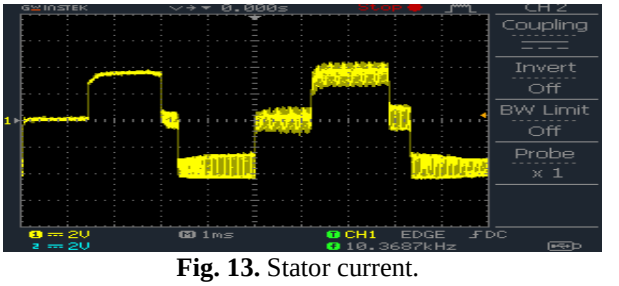

Fig. 13. Stator current.

Figs. 14-16 show the intermittent cut-off signals from three commutation signals by PWM inverter.

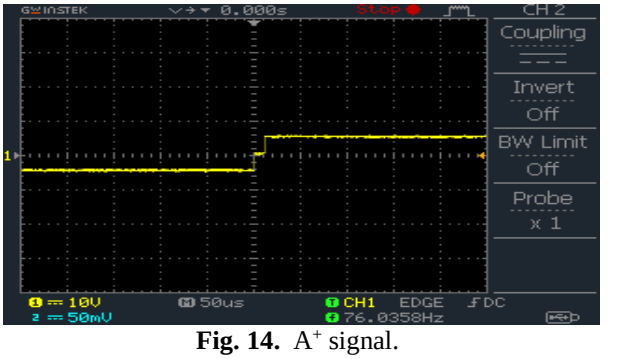

Fig. 14. A^+ signal.

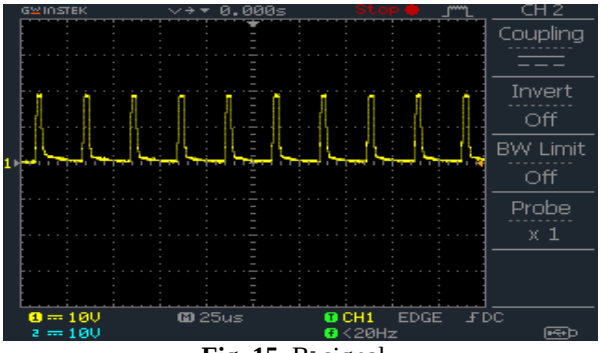

Fig. 15. B^- signal.

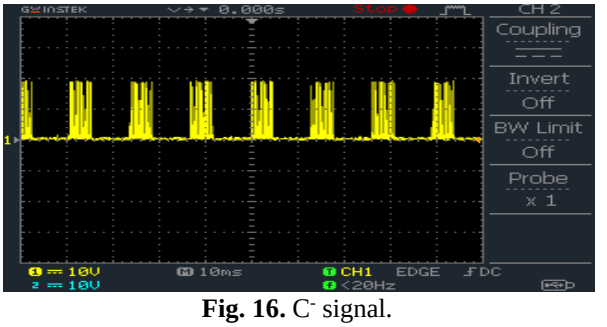

Fig. 16. C^- signal.

In Fig. 17 output pulses of two drives (IR2101) is illustrated. It can be seen that the off – on command from both drives is not sent to the fire circuit at the same time.

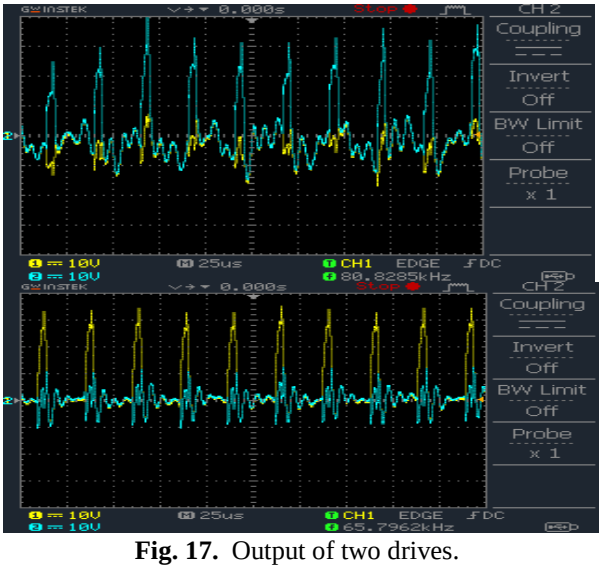

Fig. 17. Output of two drives.

Fig.18 shows the waveform of the two motor phases. It can be seen that phase charging and discharging process is accomplished at high speed to keep the motor operation in the desired speed.

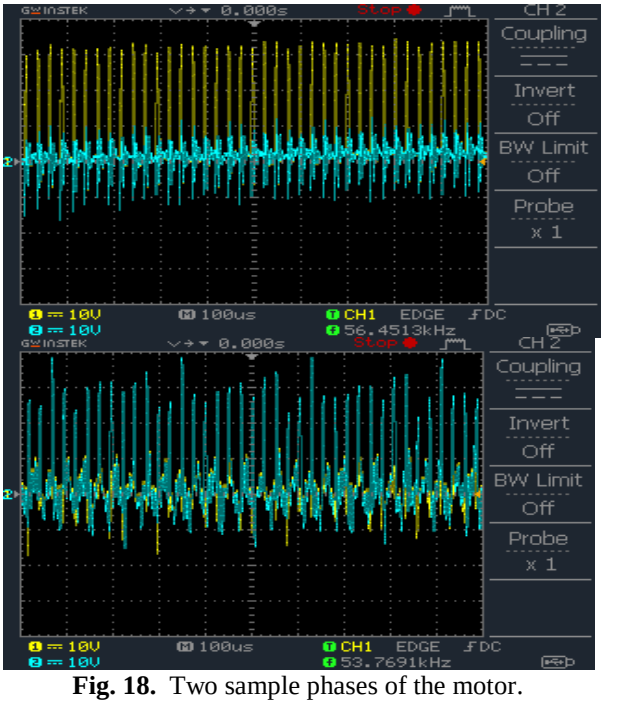

Fig. 18. Two sample phases of the motor.

Fig. 19 shows the waveforms between the first MOSFET and the first phase, and the second MOSFET and the second phase which represents the on-off command of phases.

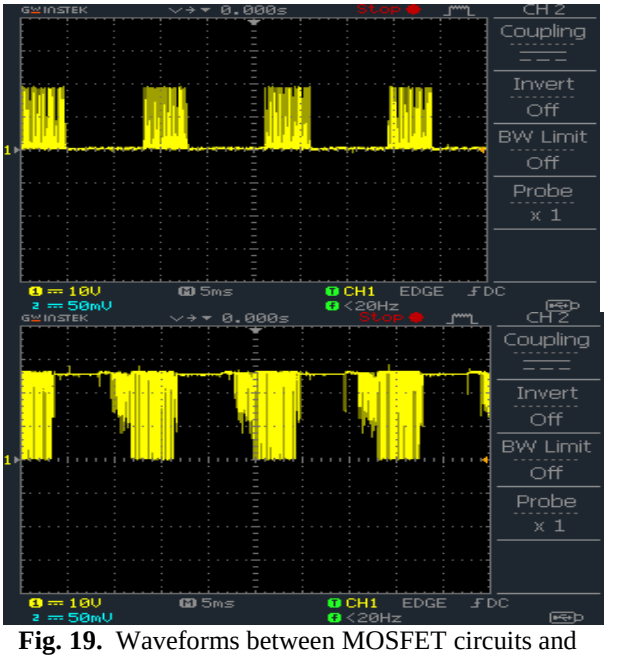

Fig. 19. Waveforms between MOSFET circuits and phases A and B.

In this paper, the simulation and the experimental results are provided to verify the validation of the proposed method. It can be seen that in the proposed

scheme, the simulation results and the experimental results are almost the same.

5. CONCLUSION

In this paper, a BLDC motor is controlled using a sensorless method. The control method applied is hysteresis comparator which enables noise and torque ripple reduction and elimination in terminal voltage. Also, this comparator is effective in phase delay compensation of back EMFs. In addition, the stator current can be easily adjusted by modulating the pulse width of the switching devices. In our proposed method, a sensorless drive is considered where the hardware complexity and the motor size are reduced and high reliability is gained. Since the number of transistors is reduced, cost reduction is gained in the proposed method comparing with sensored/sensorless BLDC conventional drives. Also, in the proposed method, the torque per volume is improved comparing with sensored/ sensorless BLDC conventional drives, so efficiency is improved in the same torque per volume. Also, the motor is able to work in environments with high temperature, humidity and high pollution, since it is sensorless. The simulation and the experimental results demonstrate the superior performance of the proposed motor drive.

5. ACKNOWLEDGEMENT

The authors gratefully acknowledge the financial and other support of this research, provided by Young Researchers and Elite Club, Islamshahr Branch, Islamic Azad University, Islamshahr, Iran.

Nomenclature

n	Resistance ratio
t_a	Time delay between $\frac{T_s}{12}$ and t_c
t_c	Time between V_p and u_{cf}
T_s	Terminal voltage period
u_{cf}	Phase C filtered terminal voltage
V_{da}	Phase A differential voltage of hysteresis comparator
V_{LT}	Minimum of the phase C terminal voltage
V_{oa}	Phase A differential voltage of the hysteresis comparator output
V_p	Terminal voltage peak
V_{sat}	Output voltage level
V_{UT}	Maximum of the phase C terminal voltage
Z_a	Phase A commutation signal
Z_b	Phase B commutation signal
Z_c	Phase C commutation signal
Greek symbols	
θ_a	Phase difference of the three commutation signals from the commutation points estimated by three-phase terminal voltages

REFERENCES

[1] E. Afjei, O. Hashemipour, M. Saati, M. Nezamabadi, **"A New Hybrid Brushless DC Motor/Generator Without Permanent Magnet",** *International Journal of Engineering Transactions B Applications*, Vol. 20, No. 1, pp.77-86, 2007.

[2] M. Pourjafari, E. Fallah Choolabi, M. Jafarboland, **"Optimum Design of Brush- Less DC Motor with Minimum Torque Pulsation Using FEM& PSO",** Amirkabir *University of Technology (Tehran Polytechnic)*, Vol. 44, No. 2, pp. 59- 70, 2012.

[3] B.K. Lee, T.H. Kim, M. Ehsani, **"On the Feasibility Of Four-Switch Three-Phase BLDC Motor Drives For Low Cost Commercial Applications: Topology And Control,"** *IEEE Trans. Power Electron.,* Vol. 18, No. 1, pp. 164-172, 2003.

[4] S., Ogasawara, H. Akagi, **"An Approach to Position Sensorless Drive for Brushless DC Motors,"** *IEEE T IND APPL,* Vol. 27, No. 5, pp. 928-933, 2001.

[5] B. K. Lee, J.P. Hong, M. Ehsani, **"Generalized Design Methodology of Reduced Parts Converters for Low Cost BLDC Motor Drive,"** *in Proc. 2003 Eighteenth Annual IEEE Applied Power Electronics Conference and Exposition, APEC '03,* pp. 277-280.

[6] N. Ertugrul and P. Acarnley, **"A New Algorithm for Sensorless Operation of Permanent Magnet Motors,"** *IEEE T IND APPL,* Vol. 30, No.1, pp. 126-133, 1994.

[7] H. Takashima, M. ITA, Z. Chen, M. Satoh, S. Doki, S. Okuma **"Sensorless Position and Velocity Control of Cylindrical Brushless DC Motor at Low Speed Using Eddy",** *in Proc. of the power Conversion Conference, PCC Osaka,* pp. 1300-1303, 2002.

[8] W. Juan, M. Dixon, H. Rodrigo, **"Simplified Sensorless Control for BLDC Motor, Using DSP Technology,"** Presented at the *19th Electric Vehicle Symposium, EVS-19,* pp. 1431-1442, 2002.

[9] T.H. Kim, M. Ehsani, **"An Error Analysis of the Sensorless Position Estimation for BLDC Motors,"** *in Proc. 38th IAS Annual Industry Applications Conf.,* pp. 611-617, 2003.

[10] T.H. Kim, M. Ehsani, **"Sensorless Control of the BLDC Motor from Near-Zero to High Speeds,"** *IEEE Trans. Power Electron.,* Vol. 19, No. 6, pp. 1635-1645, 2004.

[11] B. Terzic, M. Jadric, **"Design and Implementation of the Extended Kalman Filter for the Speed and Rotor Position Estimation of Brushless DC Motor,"** *IEEE T IND ELECTRON,* Vol. 48, No. 6, pp. 1065-1073, 2001.

[12] T.W. Chun, Q.V. Tran, H.H. Lee, H.G. Kim, **"Sensoless Control of BLDC Motor Drive for an Automotive Fuel Pump Using a Hysteresis**

Comparator," *IEEE Trans. Power Electron.,* Vol. 29, No. 3, pp. 1382 – 1391, 2014.

[13] Z. Chen, M. Tomita, S. Doki, S. Okuma, **"New Adaptive Sliding Observers for Position and Velocity-Sensorless Control of Brushless DC Motor,"** *IEEE T IND ELECTRON,* Vol. 47, No. 3, pp. 582-591, 2000.

[14] A. Karimi Pouya, **"Design of Adaptive Neural Fuzzy Controller for Speed Control of BLDC Motors,"** *Majlesi journal of Electrical Engineering*, Vol.11, No.1 , 2017.

[15] M. Cunkas, O. Aydoğdu, **"Realization of Fuzzy Logic Controlled Brushless Dc Motor Drives Using Matlab/Simulink,"** *MATH COMPUT APPL*, Vol. 15, No. 2, pp. 218-229, 2010.

[16] R.S. Nur, **"Simulation of A Variable Speed Brushless DC Motor Using Neural Network Controller,"** *Maters thesis, University Of Tun Hussein, Malaysia*, 2011.

[17] P. Devendra, K. Alice Mary, Ch. Saibabu, **"Design and Implementation Methodology for Rapid Control Prototyping of Closed Loop Speed Control for BLDC Motor,"** *Journal of Electrical Systems and Information Technology*, 2017.

[18] M.Salehifar, M. Moreno-Equilaz, **"Fault Diagnosis and Fault-Tolerant Finite Control Set-Model Predictive Control of a Multiphase Voltage-Source Inverter Supplying BLDC Motor,"** *ISA T*, Vol. 60, pp. 143-155, 2016.

[19] M. Shirvani Boroujeni, G.R. Arab Markadeh, J. Soltani, **"Torque Ripple Reduction of Brushless DC Motor based on Adaptive Input-Output Feedback Linearization,"** *ISA T*, Vol. 70, pp. 502-511, 2017.

[20] C.L. Xia, **Permanent Magnet Brushless DC Motor Drives and Controls.** *Singapore: John Wiley & Sons Singapore Pte. Ltd*., 2012.